N90-29902

COMPUTER SIMULATION AND DESIGN OF A THREE DEGREE-OF-FREEDOM SHOULDER MODULE

D. Marco
Dept. of Mech. Engineering
Naval Postgraduate School
Monterey Ca. 93943

L. Torfason
Dept. of Mech. Engineering
Univ. of New Brunswick
Fredericton, N.B.

D. Tesar
Carol Cockrell Curran Chair in Engineering
Dept. of Mech. Engineering
Univ. of Texas at Austin
Austin, Tx.

ABSTRACT

This paper presents an in-depth kinematic analysis of a three degree-of-freedom fully-parallel robotic shoulder module. The major goal of the analysis is to determine appropriate link dimensions which will provide a maximized workspace along with desirable input to output velocity and torque amplification. First-order kinematic influence coefficients which describe the output velocity properties in terms of actuator motions provide a means to determine suitable geometric dimensions for the device.

Through the use of computer simulation, optimal or near optimal link dimensions based on predetermined design criteria are provided for two different structural designs of the mechanism. The first uses three rotational inputs to control the output motion. The second design involves the use of four inputs, actuating any three inputs for a given position of the output link. Alternative actuator placements are examined to determine the most effective approach to control the output motion.

1. INTRODUCTION

Recent attention has been given to an alternative to serial robotic architecture. Designs based on closed loop kinematic chains or parallel architecture are currently under investigation. The general idea of parallel design is that the output body is controlled by a combination of mutually supportive constraints. Specifically, the structural links and input actuators all act together, directly influencing the motion of the output body. This method provides improved structural rigidity, precision positioning, and favorable load distribution [1].

The shoulder module shown in Figure 1 is a purely spherical device using three inputs. It has been conceived to precisely control three rotational degrees-of-freedom. Since the device kinematically mimics a ball-and-socket joint, no translational freedoms are present. The design has been examined and analyzed in [2,3]. Included in these references are the derivation of the first and second-order influence coefficients needed to describe the velocity and acceleration characteristics of the system, along with some preliminary optimization work.

The shoulder may be used as a component for a six degree-of-freedom force feedback joystick controller [4]. The joystick structure consists of the shoulder at the base, connected to a chain of three revolute joints with the operator gripper located at the end of the chain. Since force-feedback controllers require actuators to apply reflective forces on the operator, it is of utmost importance to design the controller to be as light as possible. This will minimize operator effort and fatigue. Locating the shoulder at the base will enable three of the actuators to be fixed to ground. Therefore, not representing any mass to the moving system. The shoulder may also serve as the base component for a combination serial/parallel manipulator [5]. In this case, locating the three shoulder drives on the ground will greatly reduce link deflections as well as inertial effects associated with purely serial architectures.

The primary objective of this work is to obtain suitable mechanism dimensions for the shoulder module based on predetermined design criteria. Link dimensions which provide uniform torque and velocity transmission from input to output are sought. Since the velocity and torque are inversely proportional at constant power, it is desired to obtain an equal balance between the two. Achieving this balance will ensure ease of actuator speed control as well as reduction of the actuator torque requirements. In most robotic systems,the region of the workspace in which the manipulator has adequate performance characteristics is considerably smaller than the overall workspace. Therefore, maximization of favorable operating regions is also desired.

Determination of the most effective actuation strategy is clearly of importance.Currently, the shoulder is conceptualized to be actuated by rotational inputs on the base as shown in Figure 1.

Section 2 briefly outlines the geometric and kinematic description of the device, with the available dimensions for design optimization. Section 3 outlines the design methodology used to establish the performance criterion. Sections 4 and 5 present the results of optimization for two different structural designs. Described in the sixth section are alternative actuation schemes which determine the best input strategies. The final section presents results and concluding remarks.
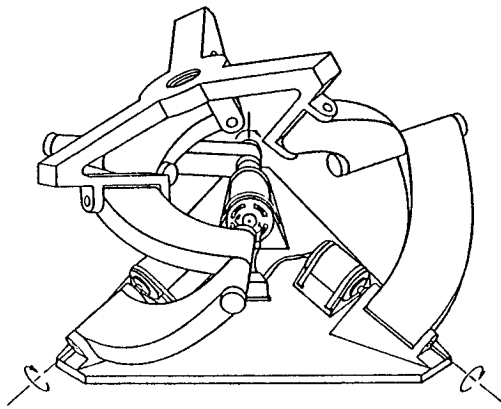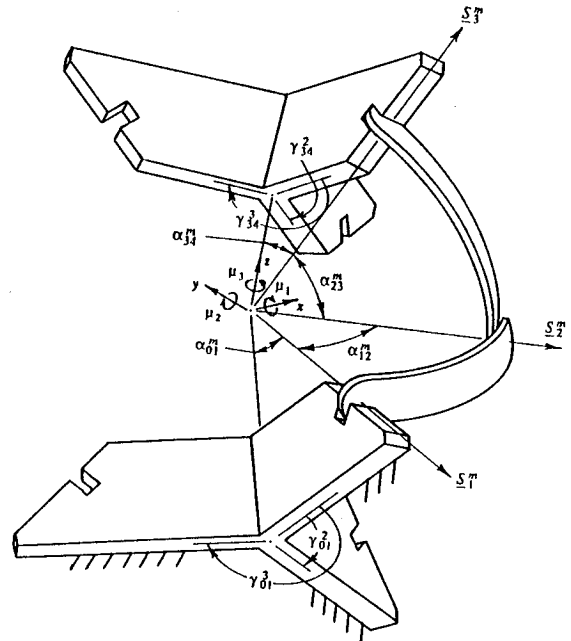

Figure 1 The Shoulder Module

Figure 2 Shoulder Geometric Description

2. SHOULDER MODULE GEOMETRIC AND KINEMATIC DESCRIPTION

The design consists of two tetrahedrons connected by three spherical binary link pairs or "dyads". Only one dyad is shown in Figure 2 for clarity. The upper tetrahedron is the moving or output link which possesses the three rotational degrees of freedom. The lower tetrahedron is the base or ground link. Each dyad chain is made up of two spherical links and three revolute joints driven by a separate actuator located on the base joint.

In order to produce purely spherical motion, all nine joint axes must intersect at a common point. For each dyad, the revolute joint axes directions are denoted by $\underline{S}_n^m$. The superscript, m, corresponds to the subchain or dyad being described, while the subscript, n, denotes a particular joint in the subchain. There are three subchains and three joints per chain.

To uniquely define the orientation of the output link, successive rotations about the respective x, y, z body fixed axes of the output link are performed. The origin of both the global and moving (body fixed) coordinate systems are located at the intersection of the nine joint axes. Initially, both the global and moving coordinate systems are coincident with each other . Then the output link is first rotated about the x-axis to define

rotation angle μ_1. This is followed by a rotation μ_2 about the resulting y-axis, and finally a rotation μ_3 about the resulting z-axis. At the workspace center, $\mu_1 = \mu_2 = \mu_3 = 0$. This orientation will be refered to as the reference position.

The twist angles of the dyad links α_{12}^m and α_{23}^m are the fixed angles between joints $\underline{S}_1^m$ and $\underline{S}_2^m$, and $\underline{S}_2^m$ and $\underline{S}_3^m$ respectively. Along with the twist angles are the apex angles. These angles describe the geometry of the upper (output link) and the lower (ground link) tetrahedrons given by α_{34}^m and α_{01}^m. The second set of angles needed to describe the links are the edge displacement angles, γ_{34}^m and γ_{01}^m. These angles define the relative angular position of the edge planes of the links as shown.

In general there are sixteen parameters required to completely describe the geometry of the shoulder, six twist, six apex, and four non-zero edge displacement angles. They make up the complete set of variables available for optimization. If symmetry of the device is exploited, the sixteen required parameters reduce to only four. In this case, all dyads are identical and each tetrahedron is symmetrical (i.e. each edge plane is spaced 120° apart).

The relationship between the input actuator speeds and the output ternary velocity is [2]:

$$\underline{\dot{u}} = [G_\phi^u]\underline{\dot{\phi}} \tag{1}$$

where $\underline{\dot{\phi}}$ is the vector of input actuator speeds which is the time derivative of each input angular displacement, and $\underline{\dot{u}}$ is the output link angular velocity expressed in a global reference. $[G_\phi^u]$ is the influence coefficient matrix or Jacobian where the superscript, u, refers to the dependent variable, while the subscript, ϕ, denotes the independent variable [6,7]. The Jacobian is defined by

$$[G_\phi^u] = \frac{\partial \underline{\dot{u}}}{\partial \underline{\dot{\phi}}} = \begin{bmatrix} \dfrac{\partial \underline{\dot{u}}}{\partial \dot{\phi}_1} & \dfrac{\partial \underline{\dot{u}}}{\partial \dot{\phi}_2} & \dfrac{\partial \underline{\dot{u}}}{\partial \dot{\phi}_3} \end{bmatrix} \tag{2}$$

where the ith component of Equation (2) is

$$[G_{\phi i}^u] = \begin{bmatrix} \partial \dot{u}_x / \partial \dot{\phi}_i \\ \partial \dot{u}_y / \partial \dot{\phi}_i \\ \partial \dot{u}_z / \partial \dot{\phi}_i \end{bmatrix} \tag{3}$$

The x, y, and z subscripts in Equation (3) refer to the x, y, and z components of $\underline{\dot{u}}$ expressed in a global reference.

The Jacobian, $[G_\phi^u]$, can be used to obtain the input torque requirement, $\underline{T}_\phi$, for a given applied load state, $\underline{T}^u$, using a virtual work formulation. $\underline{T}_\phi$ is a three component vector of the input actuator torques along the $\underline{S}_1^1$, $\underline{S}_1^2$, and $\underline{S}_1^3$ axes. These are the torques required to counteract the applied loads on the output link to maintain the system in static equilibrium. For static equilibrium, the virtual work, δW, must be zero, therefore

$$\delta W = \underline{T}_\phi \cdot \delta \underline{\phi} + \underline{T}^u \cdot \delta \underline{u} = 0 \tag{4}$$

where the virtual output displacements, $\delta \underline{u}$, must conform to the constraints of the system. From Equation (1)

$$\delta \underline{u} = [G_\phi^u]\delta \underline{\phi} \tag{5}$$

since,

$$\delta \underline{u} = \underline{\dot{u}}\,\delta t$$
$$\delta \underline{\phi} = \underline{\dot{\phi}}\,\delta t \tag{6,7}$$

Subtituting Equation (5) into Equation (4), the following result is obtained

$$\underline{T}_\phi = -[G^u_\phi]^T \underline{T}^u = -\underline{T}^L_\phi \tag{8}$$

where $\underline{T}^L_\phi$ is defined as the effective load at the input $\underline{\phi}$ due to loads applied to the output link.

3. SHOULDER DESIGN METHODOLOGY

In order to establish the required design method based on the input and output velocity relationship, the Rayleigh quotient is used . For a symmetric matrix [A], the quotient is stated as

$$R(\underline{x}) = \frac{x^T[A]x}{\underline{x}^T\underline{x}} \tag{9}$$

The quotient $R(\underline{x})$ is minimized by the eigenvector, $\underline{x}_{min}$, corresponding to the minimum eigenvalue, λ_{min}, of [A]. Similarily, $R(\underline{x})$ is maximized by the eigenvector, $\underline{x}_{max}$, associated with the maximum eigenvalue, λ_{max}, of [A]. This places and upper and lower bound on $R(\underline{x})$ by

$$\frac{x^T_{max}[A]\underline{x}_{max}}{\underline{x}^T_{max}\,\underline{x}_{max}} = \frac{x^T_{max}\,\lambda_{min}\,\underline{x}_{max}}{\underline{x}^T_{max}\,\underline{x}_{max}} = \lambda_{max} \tag{10}$$

$$\frac{x^T_{min}[A]\underline{x}_{min}}{\underline{x}^T_{min}\,\underline{x}_{min}} = \frac{x^T_{min}\,\lambda_{min}\,\underline{x}_{min}}{\underline{x}^T_{min}\,\underline{x}_{min}} = \lambda_{min} \tag{11}$$

Therefore, for any vector $\underline{x}$

$$\lambda_{min} \le \frac{x^T[A]x}{\underline{x}^T\underline{x}} \le \lambda_{max} \tag{12}$$

Recalling Equation (1) it is desired to obtain an upper and lower bound for the output velocity, $\underline{\dot{u}}$, and the input speeds, $\underline{\dot{\phi}}$. In order to achieve this, the ratio of the output to the input velocity magnitude is expessed as

$$\frac{\underline{\dot{u}}}{\underline{\dot{\phi}}} = \left[\frac{\underline{\dot{u}}^T\underline{\dot{u}}}{\underline{\dot{\phi}}^T\underline{\dot{\phi}}}\right]^{\frac{1}{2}} \tag{13}$$

and substituting Equation (1) into Equation (13) yields

$$\frac{\underline{\dot{u}}}{\underline{\dot{\phi}}} = \left[\frac{\underline{\dot{\phi}}^T[G^u_\phi]^T[G^u_\phi]\underline{\dot{\phi}}}{\underline{\dot{\phi}}^T\underline{\dot{\phi}}}\right]^{\frac{1}{2}} \tag{14}$$

Equation (12) may now be written as

$$(\Lambda_{min})^{\frac{1}{2}} \le \left[\frac{\underline{\dot{\phi}}^T[G^u_\phi]^T[G^u_\phi]\underline{\dot{\phi}}}{\underline{\dot{\phi}}^T\underline{\dot{\phi}}}\right]^{\frac{1}{2}} \le (\Lambda_{max})^{\frac{1}{2}} \tag{15}$$

where Λ_{max} and Λ_{min} are the maximum and minimun eigenvalues of $[G^u_\phi]^T[G^u_\phi]$. Since the performance of $\underline{\dot{u}}$ relative to $\underline{\dot{\phi}}$ is of interest, Equation (1) is back substituted into Equation (15) to obtain

$$|\dot{\underline{\phi}}|(\Lambda_{min})^{\frac{1}{2}} \leq |\dot{\underline{u}}| \leq (\Lambda_{max})^{\frac{1}{2}} |\dot{\underline{\phi}}| \tag{16}$$

Defining

$$\lambda_{max} = (\Lambda_{max})^{\frac{1}{2}}$$

$$\tag{17,18}$$

$$\lambda_{min} = (\Lambda_{min})^{\frac{1}{2}}$$

Equation (16) becomes

$$|\dot{\underline{\phi}}| \lambda_{min} \leq |\dot{\underline{u}}| \leq \lambda_{max} |\dot{\underline{\phi}}| \tag{19}$$

This formulation may also be used to obtain the extremes of the torque values. Recalling Equation (8), and applying the same procedure as before with $[G_\phi^u][G_\phi^u]^T$, the magnitude of the input and output torques are related by

$$|\underline{T}^u| \lambda_{min} \leq |\underline{T}_\phi| \leq \lambda_{max} |\underline{T}^u| \tag{20}$$

Equations (19) and (20) now provide a means to analyze the torque and velocity characteristics of the shoulder. These characteristics are described by the relative values of the maximum and minimum eigenvalues. As seen from Equation (19), large eigenvalues indicate a large velocity amplification from the input actuators to the output link. On the other hand, small eigenvalues indicate a small amplification. In contrast to the above relationship, the torque amplification is inversely proportional to the velocity amplification. This is analogous to mechanical advantage. Refering to Equation (20), large eigenvalues indicate a low torque transmission from the input to the output, and small eigenvalues signify high torque transmission.

From a practical point of view, the designer would like to have high torque transmission from input to output, for this increases payload and reduces actuator size. This leads to the assumption that small system eigenvalues are desired. However, this will sacrifice the speed of response of the device, since small eigenvalues signify a small velocity amplification. This also implies a small range of motion. Due to these characteristics, a give and take situation exists between the load capacity and operating speed. In order to have balance between the two, eigenvalues of one are desired. This is an ideal case and since the shoulder mechanism is very non-linear, it can not be achieved throughout the entire workspace.

A second justification for unity eigenvalues concerns the relative separation of the maximum and minimum eigenvalues. Both in general will not be relatively large or relatively small. The larger the separation between λ_{min} and λ_{max}, the larger the separation between the upper and lower bounds of the velocity and torque relationships. Refering to Equation (19), the magnitude of the output velocity will be at its upper limit if the input velocity vector lies along $\underline{x}_{max}$ of $[G_\phi^u]^T[G_\phi^u]$, and at its lower limit with this vector along $\underline{x}_{min}$. Similar characteristics are observed by the applied torque vector in Equation (20). When this vector lies along $\underline{x}_{max}$ of $[G_\phi^u][G_\phi^u]^T$, the required input torque is at a maximum. If the output torque vector lies along $\underline{x}_{min}$, the opposite action takes place and high torque transmission is present from the actuators to the output. This leads to a second basic design criteria: It is desired that the variance between the maximum and minimum eigenvalues be kept to a minimum.

4. DESIGN OF THE THREE DYAD SHOULDER

The maximum and minimum eigenvalues are evaluated for given output link positions throughout the workspace. In doing this, an insight into the desirable mechanism dimensions are obtained. The Jacobian is a function of the fixed geometric parameters along with the position of the output link. This suggests that by varying the fixed dimensions, (i.e. twist, apex, and edge displacement angles), the input to output relationship

can be tuned to provide suitable performance throughout the workspace. However, since the Jacobian is also a function of the output position, the input output relationship is not constant and highly non-linear, and only certain regions of the workspace will be suitable for operation.

In order to compactly represent the locations and magnitudes of the maximum and minimum eigenvalues, contour plots are generated to determine the regions of desirable operation. The eigenvalues are evaluated over an operating range of μ_1 , μ_2 , μ_3 , each from -90° to +90°. Since the three independent parameters must be represented on paper, two of the variables, μ_1 and μ_2 are evaluated over the -90° to +90° range with μ_3 held constant . μ_3 is then incremented from -90° to +90° to give an overall view of the operating range. Once the plots for each constant value of μ_3 are generated, they are overlayed, and the contour lines common to all of the plots (i.e. throughout the range of μ_3) are traced out .

After an extensive trial-and-error search for suitable link dimensions, including non-symmetric designs, near optimal values were isolated. These values determined that the design should be symmetrical. Contour plots for two representative geometries are shown in Figures 3 and 4. Comparing the plots for each case it is observed that no region of unity eigenvalues exist. This condition is approched at the workspace center (reference position), but is never attained. It is also evident that the variance between the maximum and minimum eigenvalues increases outward from the workspace center.

The eigenvalue behavior for a geometry with apex angles of 45° and twist angles of 90° is shown in Figure 3. This design provides a large, smooth region of maximum eigenvalues along with a small gradient present in the minimum eigenvalue plot. However, there are two areas of high maximum eigenvalue gradient in locations μ_1 = -36° with μ_2 = 45° and -45°. In these regions, the dyad links are becoming fully extended approaching a stationary configuration. In an attempt to remove the full extension, thereby increasing the mechanical advantage, the dyad twist angles were increased from 90° to 100° and then to 120°. This adjustment did improve the behavior in the regions described, but an overall degradation of performance was observed.
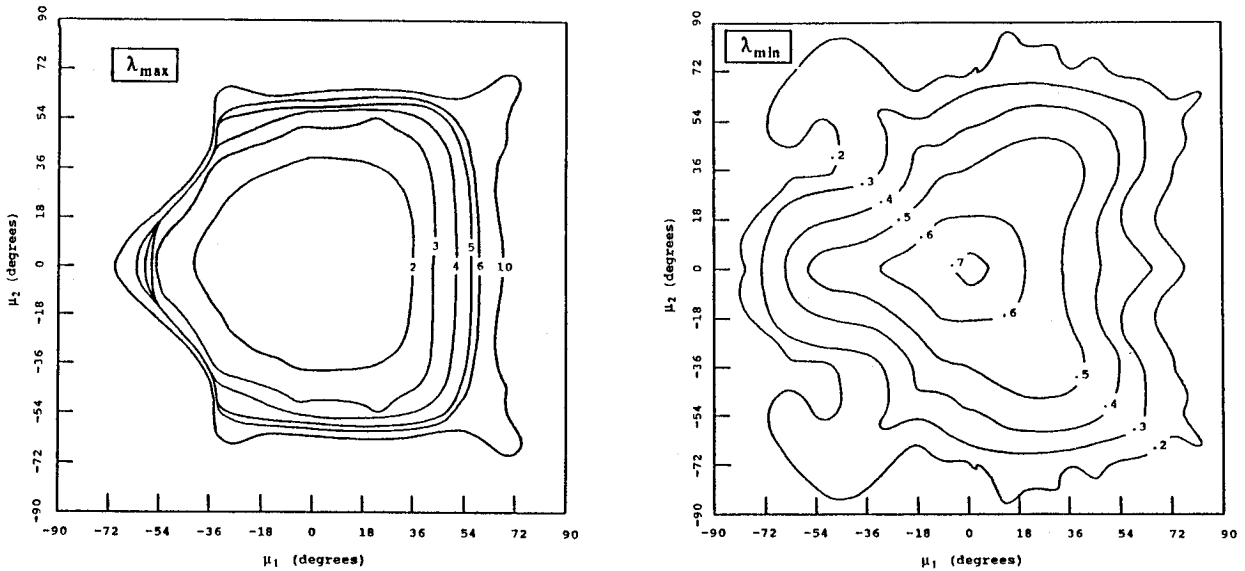

Figure 3 Maximum and Minimum Eigenvalues

Figure 4 depicts the eigenvalue behavior for apex angles of 50° and twist angles of 90°. This design has been selected as having the best overall performance characteristics. A very large, smooth area of maximum as well as minimum eigenvalues is present. The only detraction from this case is again some evidence of full extension of the links. For this set of dimensions, the extension occurs in the areas of μ_1 = -50° with μ_2 = 45° and -45°. This is not as severe as in the previous case, and since these regions occupy a small percentage of the workspace, they may be avoided during operation.
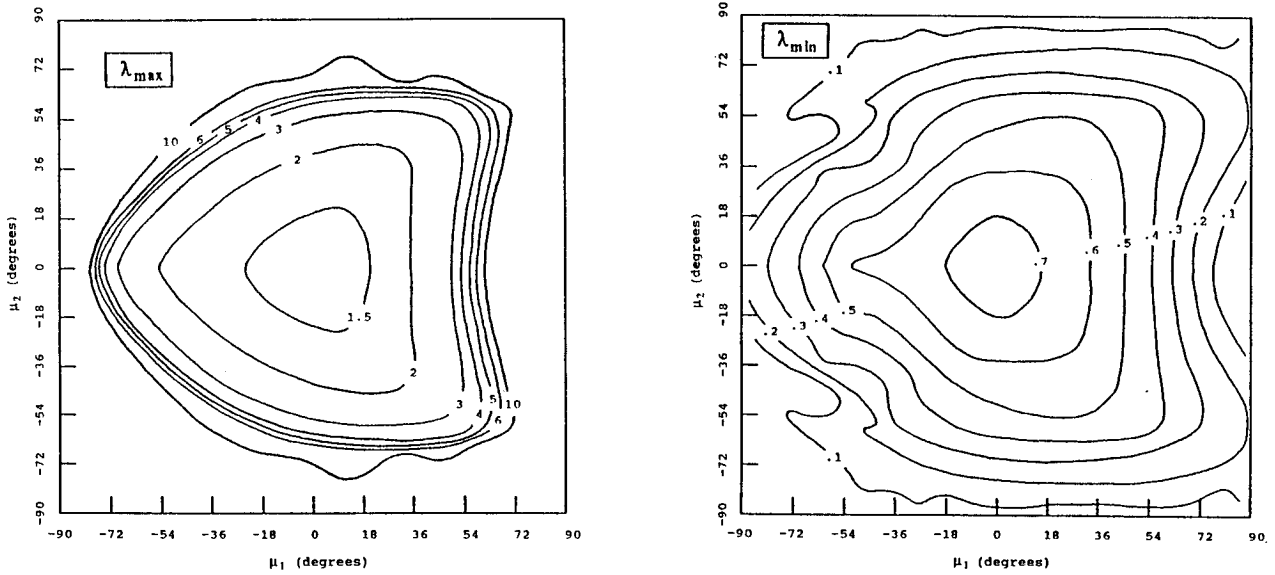
Figure 4 Maximum and Minimum Eigenvalues

5. DESIGN OF THE FOUR DYAD SHOULDER

The results of the previous section have shown the performance of the shoulder is dependent on the fixed geometric parameters. Once these values have been selected, the performance characteristics for a particular set of dimensions are invariant. It would be desirable to be able to change the mechanism dimensions during operation to adapt to the non-linear behavior of the system. Since this is not practical, a design utilizing four inputs has investigated. This design is identical to the three dyad shoulder except an additional actuated dyad has been included connecting the base link to the output link. Since the fourth dyad is geometrically identical to the other three, and its revolute joint axes also intersect at a common point, the spherical output motion will not differ from the three dyad design.

The four dyad design is shown in Figure 5. Each leg of the base and output link is spaced at 90° apart to maintain symmetry. All four dyads will not be actuated simultaneously. Since three inputs are required to position and control the output, only three of the inputs will be active at any one time. The three of four inputs which best fulfill the design criteria will be actuated to control the output motion. The fourth dyad actuator will remain inactive.
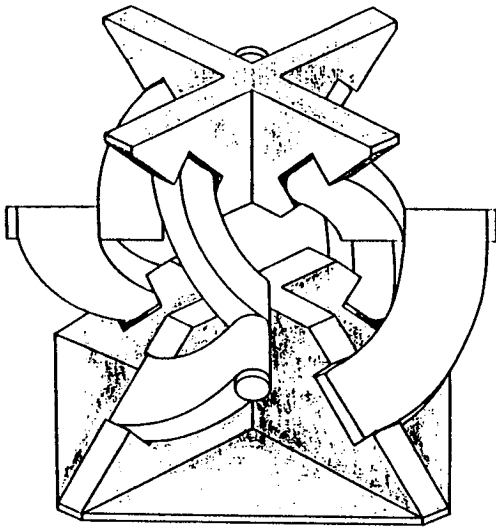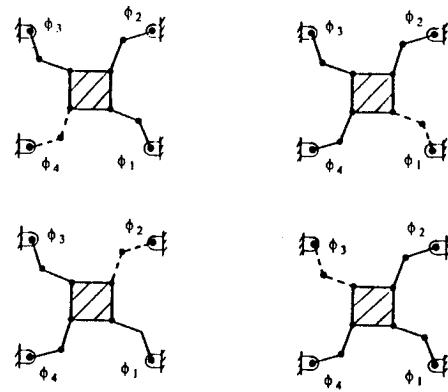

Figure 5 The Four Dyad Shoulder

Figure 6 Actuation Strategy

279

For ease of graphical representation, the planar equivalent of the device, shown in Figure 6, will be used to describe the selection of the best combination of three inputs to actuate the system. Since only three out of four can be used at any one time, the combination yielding a maximum eigenvalue nearest unity was selected. This choice is one of many, and, minimum eigenvalues could have been used. However, this makes the selection more difficult because their characteristics are more variable.
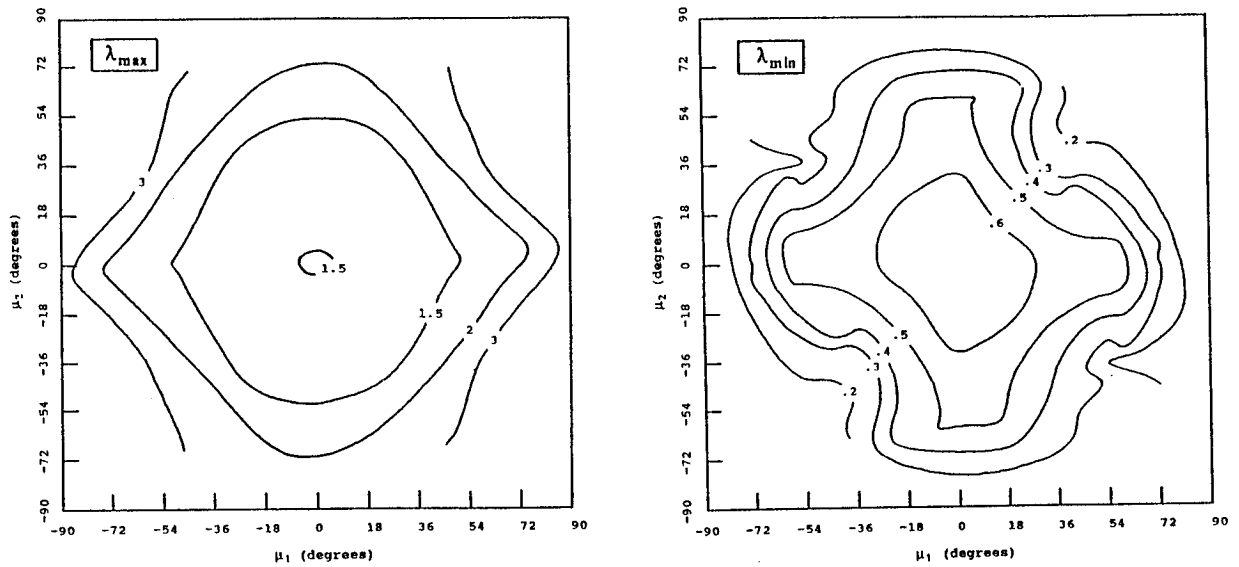

Figure 7 Maximum and Minimum Eigenvalues

The eigenvalue behavior with apex angles of 45° and twist angles of 90° is shown in Figure 7. A region of very good maximum eigenvalues exist with a smooth gradient outward from the center of the workspace. The minimum eigenvalue results were not as promising, but are relatively smooth. Strong symmetry is evident about the workspace center. This is expected due to the ability to alternate between four geometric arrangements during operation.
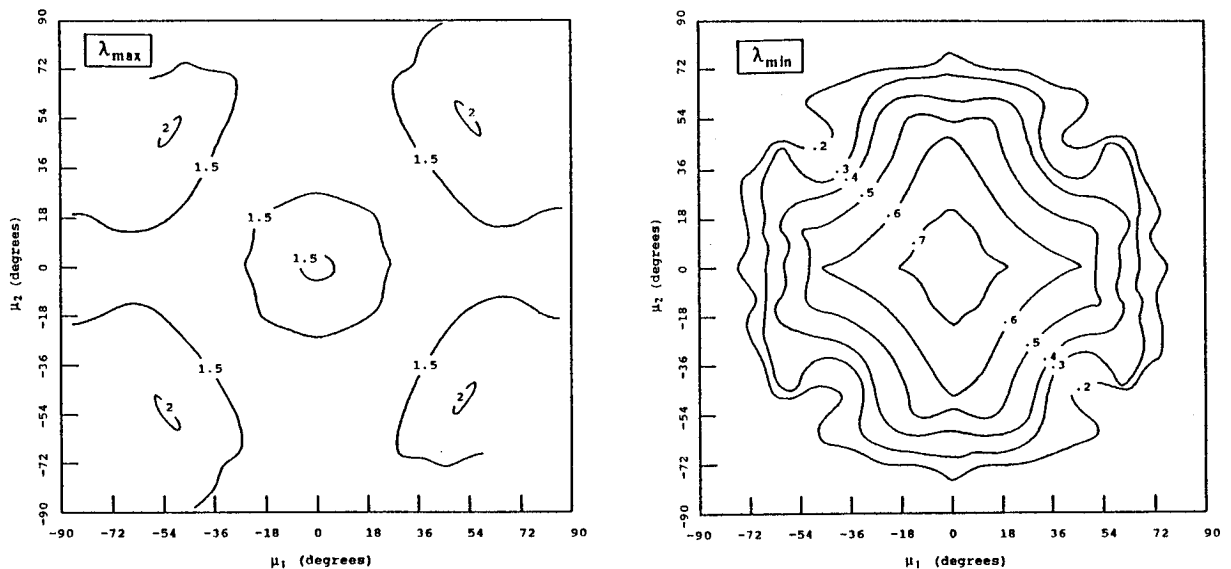

Figure 8 Maximum and Minimum Eigenvalues

Exceptional results are obtained for apex angles of 50° and twist angles of 90° shown in Figure 8. A near constant value of 1.5 is present throughout the workspace. The corresponding minimum eigenvalues also behave

remarkably well. Like the previous case, an increasing variance of the maximum and minimum eigenvalues is observed near the edges of the workspace. However, for this case the variance is relatively small. Therefore, the set of optimal mechanism dimensions selected for the three dyad shoulder has also been selected for the four dyad design.

6. ALTERNATIVE ACTUATION LOCATIONS

The method of transfer of generalized coordinates [6,7], has been applied to obtain the kinematic model relating the various inputs to the output parameters. The derivation of the kinematic model for actuating the device from any three of the joint axes is outlined in Appendix A. Various input locations were investigated, but superior results to base actuation were not found.

7. CONCLUSIONS

The analysis, simulation and geometric design of the shoulder has been presented. With the first order kinematic influence coefficients defined, a useful design tool was developed. The magnitudes of the system eigenvalues were shown to provide upper and lower bounds on the input to output velocity and torque characteristics. This prompted the search for mechanism dimensions which would provide system eigenvalues near one throughout the workspace.

Illustrative examples of maximum and minimum eigenvalue contour plots have been presented. These plots provided a good graphical representation of the system performance for various sets of mechanism dimensions. The following results have been determined for the three dyad shoulder.

Use symmetric geometries; edge displacement angles of $0°$, $120°$, $240°$ for both input and output links.

Apex angles of $50°$ for both links and dyad twist angles of $90°$ for all three dyad chains

The workspace should be limited to output orientation angles of μ_1, $\mu_2 = \pm60°$, $\mu_3 = \pm90°$.

An analysis of a four dyad shoulder was also presented. This alternative structural design proved to be better than the three dyad system. The most suitable apex and dyad twist angles were found to be identical to those of the optimal three dyad shoulder. Any three of the four available dyad chains were actuated at any one time, thus enabling the three best performing dyads to control the output for a particular position. Regions of maximum eigenvalues near one were observed throughout the workspace.

Various input locations were investigated, but superior results to base actuation were not found.

REFERENCES

1   Hunt, K. H., "Structural Kinematics of In-Parallel-Actuated Robot Arms", *ASME Journal of Mechanisms, Transmissions, and Automation in Design*, Vol. 105, 1983, pp. 705-712.

2   Cox, D. J., and Tesar, D., "The Dynamic Modeling and Command Signal Formulation for Parallel Multi-Parameter Robotic Devices", Masters Thesis, Univ. of Florida, Gainsville, FL, 1981.

3   Torfason, L., "Design of the Florida Shoulder", Internal Report, Univ. of Florida, Gainsville, FL, 1983.

4   Bryfogle, M., and Tesar, D., "The Design of a Universal Spatial Seven Degree-of-Freedom Manual Controller for Teleoperator Systems", Masters Thesis, Univ. of Florida, Gainsville, FL, 1981.

5   Sklar, M., and Tesar, D., "Dynamic Analysis of Hybrid Serial Manipulator Systems Containing Parallel Modules", *ASME Journal of Mechanisms, Transmissions, and Automation in Design*, Vol. 110, 1988, pp. 109-115.

6 Freeman, R. A., and Tesar, D., "Dynamic Modeling of Serial and Parallel Mechanisms/Robotic Systems, Part 1-Methodology", *Trends and Developments in Mechanisms, Machines, and Robotics*, DE-Vol. 15-3, 1988, pp. 7-27.

7 Freeman, R. A., and Tesar, D., "Dynamic Modeling of Serial and Parallel Mechanisms/Robotic Systems, Part 2-Applications", ibid.

8 Thomas, M., and Tesar, D., "Dynamic Modeling of Serial Manipulator Arms", *ASME Journal of Dynamic Systems, Measurement and Control*", Vol. 104, No. 3, 1982, pp. 218-228.

APPENDIX A TRANSFER OF GENERALIZED COORDINATES

The kinematic relationship between the output link velocity, $\underline{\dot{u}}$, and any set of generalized coordinates, $\dot{q}$, is given by

$$\underline{\dot{u}} = [G_q^u]\dot{q} \tag{A1}$$

The first step to obtain the influence coefficients is to model each of the three dyad chains as a separate three degree-of-freedom serial manipulator. Each manipulator consists of an upper and lower dyad link and the output link. The output link is the common output to the three manipulators. It can be shown that the Jacobian for each dyad chain, m, is given by [8]

$$[_m G_\phi^u] = [\ \underline{S}_1^m\ \ \underline{S}_2^m\ \ \underline{S}_3^m\ ] \tag{A2}$$

The velocity relationship for each chain will be

$$\begin{aligned}
\underline{\dot{u}} &= [_1 G_\phi^u]_1\underline{\dot{\phi}} \\
\underline{\dot{u}} &= [_2 G_\phi^u]_2\underline{\dot{\phi}} \\
\underline{\dot{u}} &= [_3 G_\phi^u]_3\underline{\dot{\phi}}
\end{aligned} \tag{A3}$$

$$\begin{aligned}
_1\underline{\dot{\phi}} &= (\ _1\dot{\phi}_1\ ,\ _1\dot{\phi}_2\ ,\ _1\dot{\phi}_3\ ) \\
_2\underline{\dot{\phi}} &= (\ _2\dot{\phi}_1\ ,\ _2\dot{\phi}_2\ ,\ _2\dot{\phi}_3\ ) \\
_3\underline{\dot{\phi}} &= (\ _3\dot{\phi}_1\ ,\ _3\dot{\phi}_2\ ,\ _3\dot{\phi}_3\ )
\end{aligned} \tag{A4}$$

In order to obtain the link output velocity, $\underline{\dot{u}}$, in terms of any three of the nine input velocities, Equations (A3) must be solved for $_m\underline{\dot{\phi}}$ by

$$^m\underline{\dot{\phi}} = [_m G_\phi^u]^{-1}\underline{\dot{u}} = [^m G_u^\phi]\underline{\dot{u}} \tag{A5}$$

The independent variable $\underline{\dot{u}}$ is common to all three equations. One may select any three particular rows from the three inverse Jacobians in Equations (A5). This will form a fourth, composite Jacobian which may be generalized to accommodate any three inputs by the following

$$\dot{q} = \begin{Bmatrix} ^m\dot{\phi}_n \\ ^m\dot{\phi}_n \\ ^m\dot{\phi}_n \end{Bmatrix} = \begin{bmatrix} [^m G_u^\phi]_{n;} \\ [^m G_u^\phi]_{n;} \\ [^m G_u^\phi]_{n;} \end{bmatrix}\underline{\dot{u}} \qquad \begin{aligned} m &= 1,2,3 \\ n &= 1,2,3 \end{aligned} \tag{A6}$$

where m refers to any leg and n to any input. The symbol n; refers to the nth row of the matrix. To obtain the desired input to output relationship, Equation (A6) must be inverted as follows

$$\underline{\dot{u}} = [G_u^q]^{-1}\dot{q} = [G_q^u]\dot{q} \tag{A7}$$